ORGANOMETALLICS

pubs.acs.org/Organometallics Article

Further Exploration of Aza-Cobalt-Cyclobutenes on Co^{III}(TIM) Complexes: Reactivity and Spectroelectrochemistry

Leobardo Rodriguez Segura, Reese A. Clendening, and Tong Ren*



Cite This: https://doi.org/10.1021/acs.organomet.2c00557



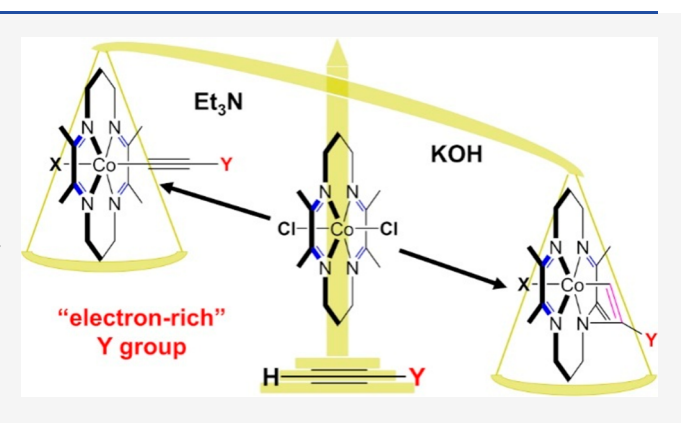
ACCESS I

III Metrics & More

Article Recommendations

s Supporting Information

ABSTRACT: The reaction between $[Co^{III}(TIM)Cl_2]PF_6$ (TIM is 2,3,9,10-tetramethyl-1,4,8,11-tetraazacyclotetradeca-1,3,8,10-tetraene) and electron-rich terminal alkynes (HC₂Y, Y = 4-N,N-bis(4-methoxyphenyl)aniline (TPA) or Fc) yielded a pair of constitutional isomers: 1-aza-2-cobalt-cyclobutene-containing trans- $[Co(TIM')((HC=C)Y)Cl]^+$ (1a (TPA) and 2a (Fc); TIM' is the resultant derivative of TIM) and σ-coordinated trans- $[Co(TIM)-(C₂Y)Cl]^+$ (1b (TPA) and 2b (Fc)). Additionally, the reactivity of the 1-aza-2-cobalt-cyclobutene species was explored based on trans- $[Co(TIM')((HC=C)Fc)Cl]PF_6$ (2a) because of its good synthetic yield. The reaction of 2a with AgOTf in MeCN resulted in trans-[Co(TIM')((HC=C)Fc)(NCMe)](PF₆)(OTf) (3), and the reaction with KCN in MeOH yielded trans- $[Co(TIM')-((HC=C)Fc)CN]PF_6$ (4). Similarly, trans-[Co(TIM)(C₂Ph)-(Co(



(CN)]PF₆ (5) was prepared from the reaction between KCN and trans-[Co(TIM)(C₂Ph)Cl]PF₆. Molecular structures of 1b and 3-5 were established through single crystal X-ray diffraction. Electrochemical studies of 2-4 revealed that these complexes display an irreversible Co^{III} reduction as well as a reversible one electron ferrocenyl oxidation between 0.11 and 0.18 V (vs Fc^{+1/0}). UV-vis spectroelectrochemical studies revealed a Co^{III} to Fc⁺ charge-transfer upon the one electron oxidation of 2a and 2b.

INTRODUCTION

Transition metal catalysts facilitate a wide variety of chemical transformations, which have been essential in advancing the field of chemistry throughout the past 50 years. While these catalysts have traditionally relied on the high activity and selectivity conferred by the noble metals (i.e., Ir, Pd, Pt, Rh, and Ru), the scarcity of these metals has inspired a growing movement to target base-metal catalysts as more earthabundant and relatively nontoxic alternatives.² In order to overcome the limitation imposed by the electronic nature of the 3d metals compared to noble metals, a leading strategy is based on using redox-noninnocent ligands to enable a twoelectron redox event instead of a one-electron event.³ In particular, Fe^{4,5} and Co^{6,7} complexes supported by pincer-type ligands, which have the ability to store electrons, have been successful in catalyzing a broad range of organic reactions including alkyne hydrogenation, olefin hydrogenation and hydrosilylation, alkyne dimerization, and the $[2\pi + 2\pi]$ cycloaddition of α , ω -dienes.

Several laboratories including ours have studied metal alkynyl complexes supported by tetra-aza macrocycle cyclam (1,4,8,11-tetraazacyclotetradecane) and its *C*-substituted derivatives, ⁸⁻¹¹ where cyclam primarily functions as a hard base ligand. More recently, studies of Fe alkynyls supported by a tetra-imine macrocycle revealed much enhanced $d\pi - \pi^*(C = N)$ interactions and the resultant intense charge transfer

bands. ^{12,13} Macrocycles containing α -diimines are potentially redox noninnocent ligands, and sequential one-electron reductions localized on the α -diimine units were demonstrated with Fe(TIM) (TIM = 2,3,9,10-tetramethyl-1,4,8,11-tetraazacyclotetradeca-1,3,8,10-tetraene) complexes. ¹⁴ Therefore, the redox noninnocence of TIM makes it an attractive target in the design of base metal catalysts. However, there is no example of a catalyst employing the TIM's ability to store two electrons to the best of our knowledge.

Our group recently reported the formation of a 1-aza-2-cobalt-cyclobutene from the reaction between $[Co(TIM)Cl_2]$ -PF₆ and electron-rich terminal alkynes $(HC_2Y, Y = DMAP (4-(N,N-dimethyl)anilino))$, Fc (ferrocenyl), or TPA (4-(N,N-bis(4-methoxyphenyl))anilino)) in the presence of KOH. Early examples of 1-aza-2-M-cyclobutenes were those of $M = Zr^{16-18}$ and Ti^{19-21} in the context of catalytic hydroamination of alkynes, and examples with M = Fe were achieved recently through a [2+2] addition of an internal alkyne across a Fe

Special Issue: Advances and Applications in Catalysis with Earth-Abundant Metals

Received: November 14, 2022



Scheme 1. Syntheses of Complexes $1-4^a$

"Conditions: (i) HC₂Y; Et₃N, MeOH; under N₂, 6–8 h. (ii) HC₂Y; KOH, MeOH; under N₂, 3–6 h. (iii) AgOTf, MeCN; under N₂. (iv) KCN, MeOH. *Isolation was not achieved via this method.

N bond. 22,23 The formation of the novel trans-[Co(TIM')-((HC=C)Y)Cl]⁺ type complexes, where TIM' is the resulting derivative of TIM (Scheme 1), is attributed here to an unexpected noninnocent behavior of the TIM ligand. In this contribution, we have sought to gain further insight into the influences of the 1-aza-2-cobalt-cyclobutene unit on the reactivity of the CoIII center via the attempted reaction of $\textit{trans-}[\dot{Co}(TIM')((HC{=}C)Fc)Cl]PF_6 \ \ (\textbf{2a})^{\bar{}} \ \ with \ \ terminal$ alkynes and potassium cyanide (KCN) under varying conditions. Furthermore, we report the spectroelectrochemical (SEC) characterization of 2a and the σ -coordinated analogue, trans-[Co(TIM)(C₂Fc)Cl]PF₆ (2b), in efforts to elaborate on the electronic properties of the two constitutionally isomeric Co^{III} complexes. It is hoped that these investigations will aid in further understanding of the nature of bonding in 1-aza-2-Mcyclobutenes and the resulting properties of the metal center contained in these relatively uncommon organometallic units.

■ RESULTS AND DISCUSSION

Synthesis. The reaction between *trans*-[Co(TIM)Cl₂]PF₆ and 1.5 equiv of HC₂TPA in the presence of Et₃N yields two constitutionally isomeric products: trans-[Co(TIM')((HC= C)TPA)Cl]PF₆ (1a) and trans-[Co(TIM)((C \equiv C)TPA)Cl]-PF₆ (1b). As previously described, 15 the formation of the isomers is indicated by the presence of both a $\nu(C \equiv C)$ frequency stretch in the IR spectrum and a $\delta(=CH_2)$ proton signal in ¹H NMR. Because the two isomers have similar solubility, an initial attempt to separate the products via recrystallization failed. Likewise, closeness in R_{ℓ} values made traditional column separation less practical. However, the 1aza-2-cobalt-cyclobutene-containing product, 1a, appears to degrade on silica. As a result, after three repeated silica column purification efforts, 1b was isolated as a light orange solid in a yield of 17%. While 1a could not be isolated from the reaction with Et₃N, it can be selectively produced from the reaction between [Co(TIM)Cl₂]PF₆ and HC₂TPA in the presence of KOH.¹⁵ Using comparable conditions, with ethynylferrocene as the terminal alkyne, 2a can be generated in modest yields. Additionally, a mixture of 2a and 2b is formed upon the addition of HC₂Fc to a methanolic slurry of [Co(TIM)Cl₂]PF₆ in the presence of Et₃N. Silica column purification can be performed to separate the two isomers.1

To investigate the reactivity of the 1-aza-2-cobalt-cyclobutene moiety, the reaction between *trans*-[Co(TIM')((HC=

C)Fc)Cl]PF₆ (2a) and LiC₂Fc was carried out (see SI for experimental details), where the degradation of 2a instead of the addition of a second -C₂Fc was indicated by the ESI-MS of the crude mixture. Alternatively, the reaction between 2a and 1.1 equiv of AgOTf under N₂ yielded *trans*-[Co(TIM')-((HC=C)Fc)(NCMe)](PF₆)(OTf) (3) within 2 h at ambient temperature. The facile removal of the chloro ligand likely reflects a *trans* effect due to the stronger donation of the alkenyl (sp^2) anion compared to typical alkynyls (sp). Filtration of the crude reaction mixture through Celite using DCM followed by recrystallization upon the addition of diethyl ether produced 3 as red crystals in 72% yield.

In order to further explore the reactivity of the cobalt center in 3, the reaction between 3 and a second terminal alkyne was attempted. When 2 equiv of HC_2Fc were combined with 3 in MeCN in the presence of either Et_3N or KOH, only degradation of 3 was observed after 24 h. Likewise, the addition of 4 equiv of an electron-deficient alkyne, $HC_2C_6F_5$, to 3 in the presence of Et_3N did not yield new product(s) after 24 h. Overall, the lack of reactivity toward alkynyls in 3 suggests the relatively high thermodynamic stability of the structurally rigid aza-cobalt-cyclobutene unit and the stronger σ -donation of the alkenyl carbanion toward Co^{III} . In comparison, the coordination of a second alkynyl to [Co-(TIM)(C_2R)((NCCH₃)]²⁺ is facile.²⁴

Interestingly, the reaction between 2a and KCN in MeOH readily produces trans-[Co(TIM')((HC=C)Fc)CN]PF₆ (4; 52%) within 10 min. While the strong field ligands CN⁻ and RC=C⁻ are isoelectronic and strong σ -donors, the reactivity of CN⁻ with the aza-cobalt-cyclobutene unit can be attributed to its better π -accepting capabilities than RC=C⁻. To study and compare the influence of the axial CN⁻ ligand on the isomeric σ -coordinated alkynyl complexes, a reaction between [Co(TIM)(C₂Ph)Cl]PF₆ and KCN in MeOH affords trans-[Co(TIM)(C₂Ph)CN]PF₆ (5; 76%).

All new compounds are low spin Co^{III} species and have been characterized extensively via ¹H NMR, UV-vis, and IR spectroscopies. Their molecular structures have been established using single crystal X-ray diffraction, and their bulk purity has been confirmed via combustion analysis.

Structure Analysis. The molecular structures for 1–5 have been established using single crystal X-ray diffraction studies. X-ray quality crystals were obtained through slow diffusion of diethyl ether into a concentrated acetonitrile solution (1b, 3,

and 5) or acetone solution (4). The structures for 1b and 3-5 are represented in Figures 1-4, respectively, while the

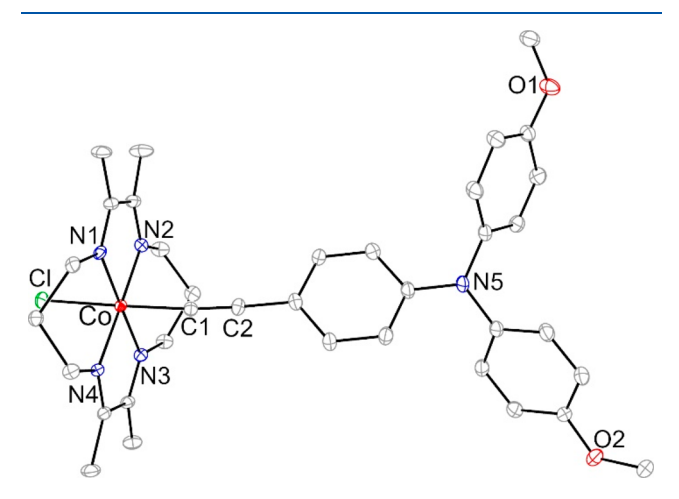


Figure 1. ORTEP plot of [1b]⁺ at 30% probability level. Hydrogen atoms and the counterions are omitted for clarity.

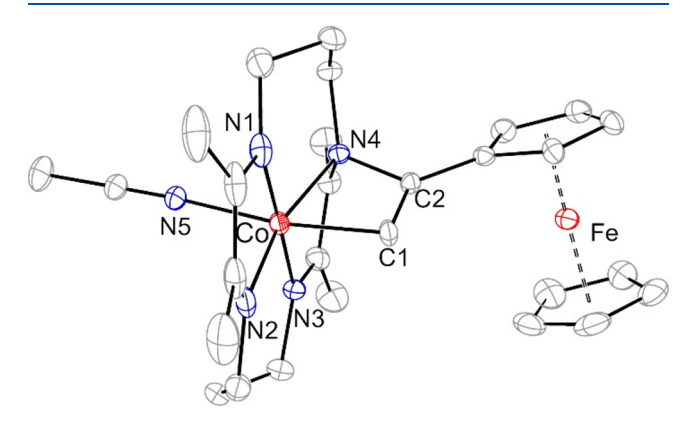


Figure 2. ORTEP plot of [3]⁺ at 30% probability level. Hydrogen atoms and the counterions are omitted for clarity.

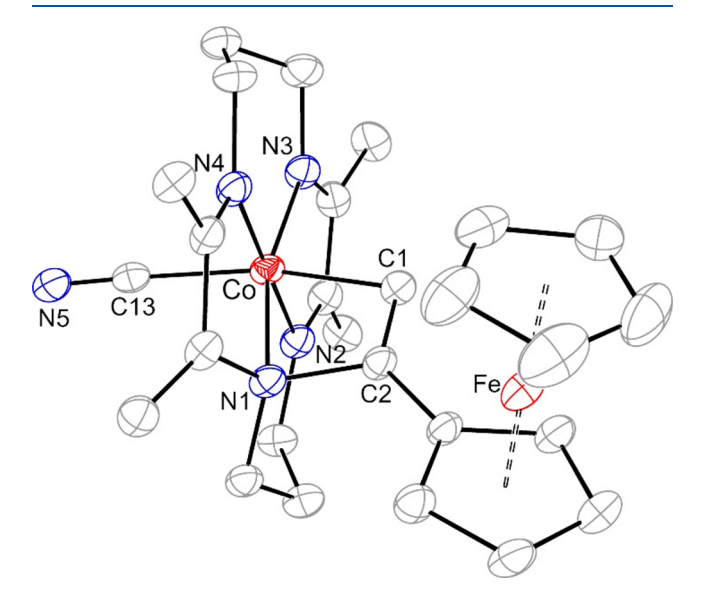


Figure 3. ORTEP plot of [4]⁺ at 30% probability level. Hydrogen atoms and the counterions are omitted for clarity.

structures for **2a** and **2b** were described in the preceding communication. Selected bond lengths and angles are

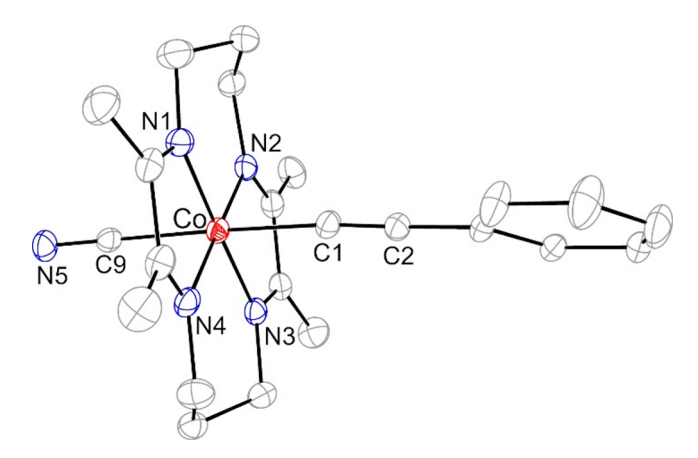


Figure 4. ORTEP plot of $[5]^+$ at 30% probability level. Hydrogen atoms and the counterions are omitted for clarity.

reported in Tables 1 and 2, and the experimental crystallographic data are provided in the Supporting Information.

Table 1. Selected Bond Lengths (Å) and Bond Angles (deg) for $[1b]^+$, $[2b]^+$, $[3b]^+$ and $[5]^+$

	[1b] ^{+a}	[2b] ⁺	[5]+
Co-N _{av}	1.916[6]	1.914[3]	1.921[7]
Co-Cl1/C9	2.294(8)	2.2907(5)	1.930(5)
Co-C1	1.884(3)	1.891(2)	1.912(5)
C1-Co-Cl1	176.63(9)	175.91(5)	176.6(2)
Co-C1-C2	171.9(3)	167.2(1)	173.1(4)
C1-C2-C3	175.8(3)	175.4(2)	175.9(5)

^aOne of the two independent molecules

Table 2. Selected Bond Lengths (Å) and Bond Angles (deg) for $[2a]^+$, $[3]^+$, and $[4]^+$

	[2a] ⁺	[3] ⁺	[4]+
Co-Cl/N5/C13	2.3438(6)	1.994(3)	1.975(6)
Co-C1	1.907(2)	1.911(3)	1.923(5)
C1-C2	1.316(3)	1.322(4)	1.319(6)
N1-C2	1.504(3)	1.499(3)	1.511(6)
N1-C14	1.454(3)	1.451(4)	1.464(6)
C14-C24	1.331(3)	1.323(5)	1.328(8)
Co-C1-C2	97.9(2)	96.7(2)	97.1(4)
C1-C2-C3	132.8(2)	132.8(3)	133.4(5)
C1-C2-N1	104.6(2)	105.3(2)	104.7(4)

Similar to the previously reported monoalkynyl $Co^{III}(TIM)$ complexes, 24 complex ${\bf 1b}$ adopts a pseudo-octahedral geometry around Co with the TIM macrocycle occupying the equatorial plane and the alkynyl and chloro ligands coordinating *trans* to one another in the axial positions. The Co–Cl bond lengths in ${\bf 1b}$ and ${\bf 2b}$ are 2.2924(8) and 2.2907(5) Å, $^{1.5}$ respectively, and are slightly elongated relative to that in *trans*-[Co(TIM)-(C₂Ph)Cl]PF₆ (2.286(2) Å). 24 This can be explained by the fact that both $^{-}$ C₂TPA and $^{-}$ C₂Fc are stronger donors than $^{-}$ C₂Ph, which results in an increased *trans* influence across the cobalt center. While the ferrocenyl moiety is expected to be electron richer than the $^{-}$ C₂TPA ligand, the slightly shortened $^{-}$ Co—C(\equiv C) bond in $^{-}$ Bb (1.883(3) Å) relative to that in $^{-}$ Bb (1.891(2) Å) is likely due to the steric bulk of the ferrocenyl unit.

The molecular structures of 3 and 4 differ from 1b, since the former feature a 1-aza-2-cobalt-cyclobutene unit. While the Co centers adopt a pseudo-octahedral geometry with the nitrogen centers lying in the equatorial plane, the axial coordination sites are occupied by an alkenyl and either an acetonitrile (3) or cyano (4) ligand. As discussed elsewhere, 15 the addition of an alkyne across the Co-N bond results in the conversion of the alkyne to an alkene as well as the formation of a carbon-nitrogen bond between the alkenyl and a TIM nitrogen. Additionally, the N1 imine is converted to an amine and the adjacent methyl converts to a methylene (see Scheme 1 for TIM'). These structural rearrangements have been verified through the analysis of the bond lengths and angles in *trans*-[Co(TIM')((HC=C)DMAP)Cl]PF₆ and 2a. 15

The two sp²-hybridized carbon atoms within the 1-aza-2-cobalt-cyclobutene unit in 2a enable the planarity of the ring, which was observed in an iron azametallacyclobutene as well. However, 2a has significantly contracted Co—C(=C) and alkene bonds of 1.907(2) and 1.316(3) Å, respectively, relative to the Fe species, which has an Fe—C(=C) bond length of 1.999(2) Å and an alkene bond length of 1.398(3) Å (see Table 3). This may be attributed to the increased steric effects

Table 3. Selected Bond Lengths (Å) and Bond Angles (deg) for Fe, ²² Ti, ²¹ and Zr¹⁷ Azametallacyclobutenes

M	Co ^{III}	Fe^{III}	$\mathrm{Ti}^{\mathrm{IV}}$	$\mathbf{Z}\mathbf{r}^{\mathrm{IV}}$
M—N	2.0083(19)	2.0083(19)	2.0372(8)	2.093(3)
M-C(=C)	1.999(2)	1.999(2)	2.1203(9)	2.203(3)
C=C	1.398(3)	1.398(3)	1.3707(13)	1.361(8)
N-C(=C)	1.370(3)	1.370(3)	1.4181(11)	1.426(5)
N-M-C	69.39(9)	69.39(9)	68.08(3)	66.33(12)
C-N-M	90.03(5)	90.03(5)	88.15(5)	90.0(3)
N-C=C	110.97(2)	110.97(2)	113.19(8)	115.1(4)
M-C=C	89.63(15)	89.63(15)	6.06(6)	87.2(2)

incurred by the coordination of an internal alkyne (1-phenyl-propyne) in the latter complex versus a terminal alkyne in 2a, which coordinates with the bulkier Fc substituent in a position β to the Co center. Consequently, the carbon–nitrogen bond in 2a is significantly elongated (1.504(3) Å). In contrast, the internal alkyne in the Fe²² species, as well as those in titanium $^{19-21}$ and zirconium 17 azametallacyclobutenes, is oriented so that the more sterically hindered substituent is in a position α to the metal center resulting in a shorter C–N bond.

Within the 1-aza-cobalt-cyclobutenes, comparison of 3 and 4 to 2a provides insight into any structural differences incurred upon the replacement of the chloro ligand with an acetonitrile or cyano group, respectively. As shown in Table 2, the Co-C(=C) bond length (1.911(3) Å) in 3 is the same as that in 2a (1.907(2) Å) within experimental error. This is in contrast to the trends observed in the isomeric σ -alkynyl complexes, where the displacement of the chloro ligand with an acetonitrile typically results in a significant shortening of the $Co-C(\equiv C)$ bond as a result of the reduced *trans*-influence. This disparity between the constitutional isomers can be attributed to the structural rigidity of the 1-aza-2-cobaltcyclobutene unit. On the other hand, the Co-C(=C) bond length in 4 (1.923(5) Å) is significantly elongated from those of 2a and 3, revealing that the trans-influence of the strong field cyano ligand across the cobalt center is considerably large to overcome the rigidity afforded by the 1-aza-2-cobaltcyclobutene. The strong *trans*-influence of the cyano ligand can also be observed for σ -alkynyl complex 5, which has an elongated Co—C(\equiv C) bond length of 1.912(5) Å when compared to that in *trans*-[Co(TIM)(C₂Ph)Cl]PF₆ (1.893(9) Å).²⁴

Additional comparison of the cyano complexes, 4 and 5, reveals a shorter $Co-C(\equiv C)$ bond in 4 compared to the $Co-C(\equiv C)$ bond in 5 by about ~ 0.01 Å. The contraction in bond length is consistent with a greater overlap between the sp²-hybridized alkenyl over the sp-hybridized alkynyl orbital and the corresponding Co orbital which results in an increased electron density at the Co^{III} center. The enhanced orbital overlap can be corroborated by the elongated $Co-C(\equiv N)$ bond for the 1-aza-2-cobalt-cyclobutene-containing product (1.975(6) Å) compared to 1.930(5) Å in 5.

The relatively long Co—C(\equiv C) bond (compared to 2a and 3) and Co—C(\equiv N) bond (compared to 5) in 4 may explain the inability of 2a to coordinate an alkynyl, as discussed above. It is clear that the addition of a second strong σ -donor results in weak axial Co—ligand bonds as a result of the mutual trans-influence exerted by each. However, the electron density at the Co can be alleviated by the π -accepting ability of the cyano ligand. In contrast, terminal alkynes tend to be both σ -and π -donors, which would exacerbate the trans-influence to the degree that the coordination of a second alkynyl moiety would be impeded. This supposition may be corroborated by examining the Co—C(\equiv CPh) bond length of [Co(TIM)-(C₂Ph)(C₂C₆F₅)]⁺ (1.928(5) Å), which is longer than that of 5 (1.912(5) Å). This implies a stronger trans-influence for even an electron deficient alkynyl compared to cyanide.

Fourier Transform Infrared Spectra (FTIR). The $\nu(C \equiv N)$ stretching frequencies of the Co^{III} complexes 4 and 5 were examined using FT-IR spectra. As shown in Figure S1, the cyano ligand in 4 has a C \equiv N stretching frequency of 2118 cm⁻¹ which is lower than in 5 (2133 cm⁻¹). This is attributed to the greater π -backbonding interactions between the Co $d\pi$ and empty $\pi^*(C \equiv N)$ upon the replacement of the alkynyl ligand in 5 with an alkenyl in 4. This is also consistent with the structural observations for the Co—C(\equiv N) bond lengths discussed above.

The influence of the cyano on the $-C_2Ph$ moiety across the Co^{III} center can also be studied by comparing the $\nu(C \equiv C)$ of the alkynyl ligand in 5 to those of $[Co(TIM)(C_2Ph)_2]PF_6$. Where the latter has a $C \equiv C$ stretching frequency of 2111 cm⁻¹, complex 5 has a $\nu(C \equiv C)$ shifted to higher energy at 2127 cm⁻¹. While both the alkyne and cyano ligands are strong σ -donors, the stronger π -accepting nature of the cyano group further alleviates the cobalt $d\pi - \pi(C \equiv C)$ antibonding interactions, which results in a stronger $C \equiv C$ bond in 5.

Fluorescence Spectroscopic Analysis. Emission spectra for compound 1a and 1b were collected at room temperature in degassed acetonitrile solutions. Table 4 lists absorption (λ_{abs}) and emission maxima (λ_{em}) in MeCN. As shown in Figure S4, the two TPA-bearing complexes have identical

Table 4. Emission Data

compound	$\lambda_{\rm abs}~({\rm nm})$	$\lambda_{\rm ex} \ ({\rm nm})$	$\lambda_{\rm em}$ (nm)
TPAC ₂ H ^a	301	301	460
1a	330	320	473
1b	319	335	475

^aIn DCM at room temperature.²⁷

emission profiles within experimental error, revealing that the mode of coordination of the alkyne (i.e., $\sigma\text{-coordinated}$ or addition across a Co–N bond) does not have any significant influence on the emissive nature of the TPA chromophore. In addition, the similarity in the emission profiles between Co^{III}TIM/TIM' complexes and TPAC₂H indicates that the emission originates from the $S_0 \rightarrow S_1$ excitation of the TPA moiety. 25,26

Electrochemistry. The voltammetric characteristics of the 1-aza-2-cobalt-cyclobutene-containing complexes, 2a, 3, and 4, were explored for the first time, and their relevant electrode potentials (vs $Fc^{+1/0}$) are listed in Table 5. For these

Table 5. Electrode Potentials of All Observed Redox Couples (V, vs Fc⁺/Fc) in 2a-4^a

	$(Co^{E_{\mathrm{pa}}}_{^{4+/3+}})$	$E_{1/2}$ (Fc ^{+1/0})	$(\operatorname{Co}^{E_{\operatorname{pc}}}_{3^{+}/2^{+}})$	$(\operatorname{TIM}^{E_{\mathrm{pc}}})$	$(\mathrm{TIM}^{E_{\mathrm{pc}}}_{-1/-2})$
2a	1.30	0.11(0.067)	-1.46	-2.38	-2.38
2b	_	0.01(0.062)	-1.06	-1.67	-2.04
3	1.51	0.18(0.062)	-1.34	_	_
4	1.39	0.12(0.062)	-1.67	_	_

"Solutions contain 1.0 mM analyte and 0.1 M n-Bu₄NPF₆ as the supporting electrolyte in MeCN. Peak separations ($E_{\rm pa}-E_{\rm pc}$) for reversible couples are shown in parentheses.

complexes, one irreversible 1 e^- reduction ($Co^{3+/2+}$) can be observed within the solvent window. The reduction for 2a occurs at -1.46 V, while the reduction of the σ -coordinated isomer 2b is anodically shifted to −1.06 V. This is consistent with the increased electron density at the Co center as a result of the electron richer alkenyl ligand in the 1-aza-2-cobaltcyclobutene-bearing complexes. Furthermore, two additional reductions are observed for the σ -coordinated monoalkynyl complex at -1.67 V and -2.04 V, which were previously assigned as being TIM-based.²⁴ However, only one additional reduction for 2a at -2.38 V is observed, which is most likely attributable to the presence of only one α -diimine unit in the 1-aza-2-cobalt-cyclobutene form (see Structure Analysis section above). The lone reduction observed at highly negative potentials is most likely localized upon the remaining α diimine unit. For the species bearing a 1-aza-2-cobalt-cyclobutene, the Co^{3+/2+} reduction is significantly influenced by the axial ligand trans to the alkenyl. In complex 3, the coordination of a neutral acetonitrile molecule results in dramatic anodic shift in the reduction potential (-1.06 V)relative to the chloro- complex as a result of a considerable amount of electron density loss at the Co^{III} center. Meanwhile, the coordination of the strong σ -donor cyano in 4 causes a cathodic shift of Co reduction to -1.67 V.

At positive potentials, a reversible $Fc^{+1/0}$ oxidation and an irreversible $Co^{4+/3+}$ oxidation are present for 2a, 3, and 4. In comparison, only a well-defined ferrocenyl oxidation can be detected for 2b within the solvent window (Figure 5). The lack of a cobalt oxidation in the latter complex further supports the increased electron density at the Co center upon the addition of the alkyne across the C-N bond, consistent with the more anodic $Co^{3+/2+}$ reduction of 2b vs 2a. Interestingly, the ferrocenyl oxidation is considerably influenced by the coordination mode and, to some extent, the identity of the axial ligand. In the σ -coordinated alkynyl complex 2b, the $Fc^{+1/0}$ oxidation potential occurs at 0.01 V. This potential is cathodically shifted from $HC \equiv CFc$ (0.16 V vs $Fc^{+1/0}$ in

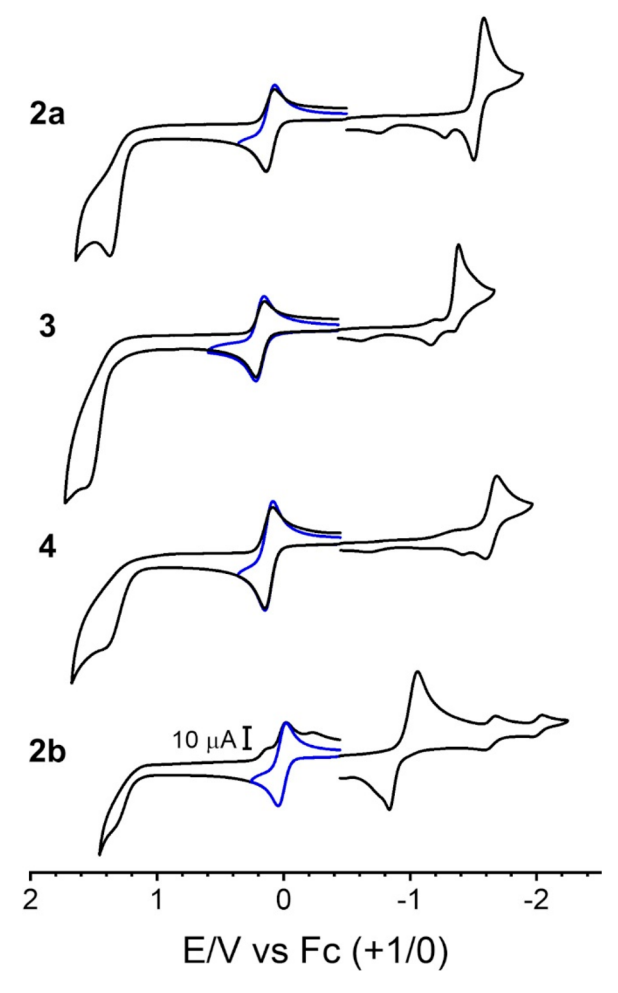


Figure 5. Cyclic voltammogram scans of 1.0 mM solutions of **2a**, **3**, **4**, and **2b** in a 0.1 M solution of $n\text{-Bu}_4\text{NPF}_6$ in MeCN at a scan rate = 0.1 V/s. Blue traces represent anodic scans up to 0.5 V.

MeCN). On the other hand, in **2a**, the ferrocenyl oxidation occurs at 0.11 V, which is positively shifted from that of $H_2C=C(H)Fc~(-0.05~V~vs~Fc^{+1/0}).^{2.8,29}$ In this case, the strong coordination between the Co^{III} center and the alkenyl moiety as well as the formation of a new C–N bond between the ethenylferrocene and the TIM ligand results in a shift of the electron density away from the ferrocenyl moiety leading to a higher oxidation potential.

The behavior of the ferrocenyl oxidation may be effectively understood by viewing the Co-X unit as a donor group. For 3, the substitution of acetonitrile for the σ/π -donating chloro results in a relatively electron-deficient Co^{III} center, and the ferrocenyl oxidation is anodically shifted (0.18 V). In 4, the coordination of the cyano ligand restores some electron density at the CoIII center and the ferrocenyl oxidation shifts to 0.12 V. This series spans only 0.07 V—in contrast to the 0.33 V span of the Co reduction potentials of these complexes because the electron density of the Co-X unit is only poorly communicated to the bulky ferrocenyl along the highly strained 1-aza-2-cobalt-cyclobutene unit. In contrast, the dramatic 0.1 V cathodic shift of the ferrocenyl oxidation in 2b compared to 2a reflects the more efficient donation of electron density along the relatively unstrained linear ethynyl bridge. This is also consistent with the 0.15 V cathodic shift in oxidation of **2b** compared to free ethynylferrocene.

Spectroelectrochemistry (SEC). In order to further probe structure-bonding relationships, SEC measurements were performed on complexes 2a and 2b in an optically transparent thin-layer electrochemical (OTTLE) cell. The SEC data for 2b (Figure 6) shows that upon oxidation the d-d transition

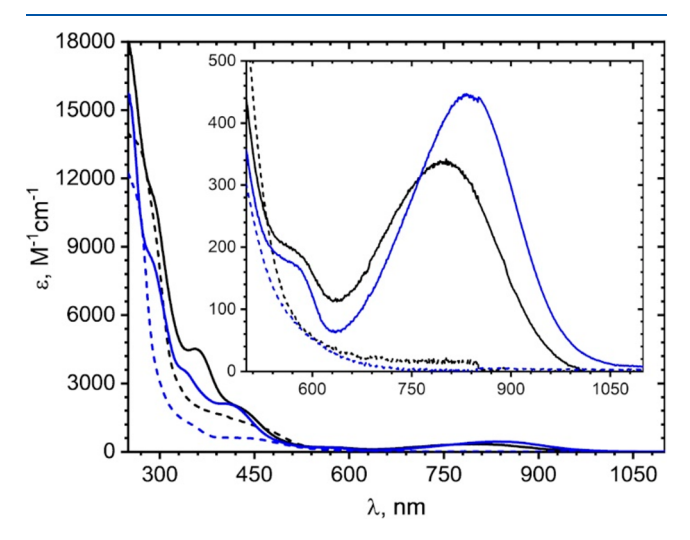


Figure 6. Absorption spectra in MeCN of **2a** in the neutral (black, dotted line) and 1e⁻ oxidized (black, solid line) states and **2b** in the neutral (blue, dotted line) and 1e⁻ oxidized (blue, solid line) states.

localized on Fc at 441 nm shifts to 412 nm and intensifies, while a new peak rises at 577 nm. These weak, complex Fcbased transitions are consistent with previous spectroelectrochemical reports on aryl-ferrocenyl dyads bridged by ethynyl or ethenyl groups.²⁸ Most significantly is the peak that rises at 835 nm with a ε of 446 M⁻¹ cm⁻¹. This transition is comparable in shape and $\lambda_{\rm max}$ to other cobalt macrocyclic complexes bearing ethynylferrocence ligands.³¹ Additionally, it resembles other metal-ethynylferrocenyl examples, namely oxidized FcC2Au and FcC2Pt species, for which this band was convincingly assigned as a metal (Pt or Au) to Fc+ charge transfer. 28,32 Furthermore, similar bands were observed for the oxidized aryl-ferrocenyl dyads already mentioned, where the energy of the transition was shown to correlate linearly with the oxidation potential of the aryl unit. Thus, the band at 835 nm in 2b⁺ is assigned as Co to Fc⁺ charge-transfer.

For the 1-aza-2-cobalt-cyclobutene isomer 2a, similar spectral changes are observed upon oxidation with the addition of a new peak at 431 nm. Notably, the charge-transfer transition at 801 nm in $2a^+$ ($\varepsilon=337~{\rm M}^{-1}~{\rm cm}^{-1}$) is weaker than that in $2b^+$. The weakening is likely attributed to geometric configuration of the 1-aza-2-cobalt-cyclobutene unit. The higher energy of this band, combined with its lower intensity, align well with the electrochemical analysis presented above. Despite the more electron-rich cobalt center in 2a, the geometric strain of the 1-aza-2-cobalt-cyclobutene bridge (combined with the bulky ferrocenyl group) hampers communication between the Co^{III} and Fc^+ centers. This is reduced by the ethynyl bridge in 2b, resulting in more favorable (lower energy and higher intensity) Co^{III} to Fc^+ charge transfer.

Some mutual electronic influence of the central Co on the ferrocenyl unit (and vice versa) may be postulated on the basis of their spatial proximity. However, the apparently poor communication between these sites implied by the SEC studies suggests that the electronic influence of the alkenyl substituent

in this position (Fc, 2a/b or TPA, 1a/b) on the Co—C(\equiv C) bond and hence the reactivity of the metal center is likely minor. The dominant force appears to be the 1-aza-2-cobalt-cyclobutene motif itself, as evidenced by the trends in reactivity and the previously reported structures. This contrasts with Co—C(\equiv C) bonding, in which the substituent appears to have a profound impact. However, a more extensive body of data would need to be compared in order to evaluate this postulation.

CONCLUSION

The successful isolation of the monoalkynyl species 1b has enabled further comparison between the two constitutional isomers. Cyclic voltammetry and spectroelectrochemistry studies of 2a and 2b were carried out, revealing significant changes in the electronic properties of the Co^{III} complexes dependent on the mode of coordination. Also noteworthy is that the strong donation from the alkenyl to the Co(III) center appears to alter the reactivity of the remaining axial site in compounds 2, as opposed to that of the Co(III) alkynyl counterparts. In addition, the facile syntheses of the new compounds 3 and 4 reveal promising opportunities to further explore the coordination of other small-molecules to the azacobalt-cyclobutene bearing complexes. Recently, directed $C(sp^2)$ -H activation by Co^{III} metallacycle complexes were demonstrated with high selectivity for ortho-alkylation.³³ Inspired by both the activity of Co^{III} metallacycle and recent developments in Co macrocyclic complexes as photocatalysts^{34,35} and copolymerization catalysts,³⁶ current efforts are underway to explore the incorporation of photocatalytic

■ EXPERIMENTAL SECTION

Materials. AgOTf was purchased from Oakwood Chemical. *n*-Butyllithium (2.5 M in hexanes) was purchased from Sigma-Aldrich. Dry acetonitrile was purchased from ACROS Chemical. All reagents were used as received. $[\text{Co(TIM)Cl}_2]\text{PF}_6$ was prepared according to literature procedures.³⁷ Also prepared according to literature procedures were 1a, 2a/b, 15 and 15 are the second control of the

Physical Measurements. UV-vis spectra were obtained with a JASCO V-780 UV-vis-NIR spectrophotometer. Emission studies were performed on a Varian Cary Eclipse fluorescence spectrophotometer in degassed MeCN solution. FT-IR spectra were measured as neat samples using a JASCO FT/IR-6300 spectrometer equipped with a ZnSe ATR accessory. ESI-MS were analyzed on an Advion LC-MS spectrometer. Elemental analysis was performed by Atlantic Microlab Inc. in Norcross, GA. ¹H NMR spectra were recorded on a Varian INOVA 300 NMR spectrometer operating at 300 MHz. Electrochemical analysis was done on a CHI620A voltammetric analyzer with a glassy carbon working electrode (diameter = 2 mm), a Pt-wire auxiliary electrode, and a Ag/AgCl reference electrode; the analyte concentration was 1.0 mM in 4 mL dry acetonitrile at a 0.1 M n-Bu₄NPF₆ electrolyte concentration. Spectroelectrochemical measurements were performed on a JASCO V-780 UV-vis-NIR spectrophotometer using an OTTLE40 liquid-sample cell with a 0.2 mm optical path length, 0.3 mL sample volume, and a CaF2 window procured from F. Hartl (Reading, U.K.). The cell was equipped with a mesh Pt working electrode, a mesh Pt auxiliary electrode, and a Ag reference electrode. The analyte concentration was 12 mM for 2a and 7.0 mM for 2b in dry acetonitrile at a 0.1 M n-Bu₄NPF₆ electrolyte concentration.

Synthesis of trans-[Co(TIM)(C_2 TPA)Cl]PF₆ (1**b**). [Co(TIM)Cl₂]PF₆ (484 mg, 0.930 mmol) was dissolved in 90 mL of a 2/1 (v/v) MeOH/acetone mixture. HC₂TPA (458 mg, 1.39 mmol) in 6.0 mL of THF was added, and the reaction mixture purged with N₂. Upon the

addition of 0.6 mL of Et₃N, the reaction turned red. After stirring for 4 h, the solvent was removed. The remaining sludge was taken up in DCM and purification over silica was attempted using a 9/1 (v/v) DCM/acetone mixture. Two subsequent attempts to purify over silica using the same solvent mixture produced **1b** as a light orange solid. Yield: 126 mg (0.154 mmol; 17% based on Co). ESI-MS [M⁺] 670.3 m/z. UV-vis, $\lambda_{\rm max}/{\rm nm}$ ($\varepsilon/{\rm M}^{-1}$ cm⁻¹): 252 (21,000), 319 (24,200), 401 (2,970). FT-IR, $\nu({\rm C} \equiv {\rm C})/{\rm cm}^{-1}$: 2126 (w). ¹H NMR (300 MHz, CD₃CN) δ 7.09–7.03 (m, 6H), 6.99–6.94 (m, 4H), 6.79–6.74 (m, 2H), 3.87 (s, 14H), 2.65–2.55 (m, 16H). Elem. Anal. Found (Calcd) for C₃₇H₄₅N₅CoCl₃O_{2.5}PF₆ (**1b**·CH₂Cl₂·0.5H₂O): C, 48.67 (48.83); H, 5.06 (4.98); N, 7.78 (7.70).

Synthesis of trans-[Co(TIM')((HC=C)Fc)NCMe](PF₆)(OTf) (3). A solution of 2a (200 mg, 0.287 mmol) in MeCN was purged with N₂ prior to the addition of AgOTf (82.0 mg, 0.316 mmol). The orange reaction mixture rapidly turned cloudy. After stirring for 2 h under N₂, the reaction was opened to air and filtered over Celite using DCM to remove the excess Ag salts. Diethyl ether was added to the orange filtrate to yield red crystals. The crystals were filtered out and washed generously with diethyl ether. Yield: 177 mg (0.208 mmol; 72% based on Co). ESI-MS [M – OTf]+ 665.2 m/z. UV–vis, $\lambda_{\rm max}/{\rm nm}$ ($\varepsilon/{\rm M}^{-1}$ cm⁻¹): 280 (11,800), 378 (2,520). FT-IR, $\nu({\rm C}{\equiv}{\rm N})/{\rm cm}^{-1}$: 2058 (w). ¹H NMR (300 MHz, CD₃CN) δ 7.82 (s, 1H), 6.17 (d, J = 3.9 Hz), 6.07 (d, J = 4.0 Hz, 1H), 4.50–3.77 (m, 17H), 3.08 (s, 2H), 2.54 (s, 11H). Elem. Anal. Found (Calcd) for C₃₀H₃₈N₅CoFeCl₂O₃SPF₉ (3· CH₂Cl₂): C, 38.65 (38.48); H, 4.23 (4.09); N, 7.06 (7.48).

Synthesis of trans-[Co(TIM')((HC=C)Fc)CN]PF₆ (4). 2a (150 mg, 0.215 mmol) was dissolved in 100 mL of MeOH and combined with a 5.0 mL solution of methanolic KCN (21.0 mg, 0.323 mmol). The reaction mixture rapidly turned from dark orange to light orange. After 10 min, the solvent was removed. The remaining sludge was taken up in DCM and washed twice with water. The organic layer was dried over Na₂SO₄. The solvent was removed, and the remaining solid was dissolved in MeCN. The addition of diethyl ether yielded 4 as an orange solid. Yield: 76.2 mg (0.111 mmol; 52% yield based on Co). ESI-MS [M⁺] 542.2 m/z. UV-vis, $\lambda_{\text{max}}/\text{nm}$ ($\varepsilon/\text{M}^{-1}$ cm⁻¹): 287 (9,970), 382 (2,120). FT-IR, $\nu(\text{C} \equiv \text{N})/\text{cm}^{-1}$: 2118 (w). ¹H NMR (300 MHz, CD₃CN) δ 8.09 (s, 1H), 6.03 (d, J = 3.8 Hz, 1H), 5.92 (d, J = 3.8 Hz, 1H), 4.40–3.78 (m, 17H), 3.04–2.87 (m, 2H), 2.49 (s, 11H). Elem. Anal. Found (Calcd) for $\text{C}_{27}\text{H}_{34}\text{N}_5\text{CoFeO}_{0.5}\text{PF}_6$ (4-0.5H₂O): C, 46.69 (46.57); H, 5.21 (4.92); N, 10.34 (10.06).

Synthesis of trans-[Co(TIM)(C₂Ph)CN]PF₆ (5). Following a similar procedure to 4, except starting from [Co(TIM)(C₂Ph)Cl]PF₆ (100 mg, 0.170 mmol) and 12.0 mg of KCN (0.184 mmol) in 5.0 mL of MeOH, yielded 5 as a yellow solid. Yield: 75.2 mg (0.130 mmol; 76% based on Co). ESI-MS [M⁺] 434.2 m/z. UV–vis, $\lambda_{\rm max}/{\rm nm}$ ($\varepsilon/{\rm M}^{-1}$ cm⁻¹): 252 (30,100), 362 (1,590). FT-IR, $\nu/{\rm cm}^{-1}$: (C≡C): 2127 (w), (C≡N): 2133. ¹H NMR (300 MHz, CD₃CN) δ 7.35–7.21 (m, 5H), 4.05 (m, 8H), 2.62 (s, 16H). Elem. Anal. Found (Calcd) for C₂₃H₂₉N₅CoClPF₆ (5): C, 47.29 (47.68); H, 5.05 (5.04); N, 12.09 (11.72).

X-ray Crystallographic Analysis. Single crystals of 1b, 3–5 were grown via slow diffusion of diethyl ether into either an MeCN solution of 1b, 3, and 5 or acetone solution of 4. X-ray diffraction data were obtained on a Bruker Quest diffractometer with Mo K α radiation (λ = 0.71073 Å) at 150 K for 1b, 3, and 5, and with Cu K α radiation (λ = 1.54178 Å) at 150 K for 4. Data were collected; reflections were indexed and processed using APEX3 and reduced using SAINT.³⁹ The space groups were assigned and the structures were solved by direct methods using XPREP within the SHELXTL suite of programs, ^{39,40} and refined using SHELX and SHELXL.^{40,41}

ASSOCIATED CONTENT

Supporting Information

The Supporting Information is available free of charge at https://pubs.acs.org/doi/10.1021/acs.organomet.2c00557.

Experimental crystallographic details; IR spectra for 4 and 5; absorption spectra for 1b and 3-5; emission

spectra for 1a and 1b; cyclic voltammograms for 5; and ¹H NMR spectra for compounds 1b and 3-5 (PDF)

Accession Codes

CCDC 2157218 and 2218109—2218111 contain the supplementary crystallographic data for this paper. These data can be obtained free of charge via www.ccdc.cam.ac.uk/data_request/cif, or by emailing data_request@ccdc.cam.ac.uk, or by contacting The Cambridge Crystallographic Data Centre, 12 Union Road, Cambridge CB2 1EZ, UK; fax: +44 1223 336033.

AUTHOR INFORMATION

Corresponding Author

Tong Ren – Department of Chemistry, Purdue University, West Lafayette, Indiana 47907, United States; ⊚ orcid.org/ 0000-0002-1148-0746; Email: tren@purdue.edu

Authors

Leobardo Rodriguez Segura — Department of Chemistry, Purdue University, West Lafayette, Indiana 47907, United States

Reese A. Clendening – Department of Chemistry, Purdue University, West Lafayette, Indiana 47907, United States

Complete contact information is available at: https://pubs.acs.org/10.1021/acs.organomet.2c00557

Notes

The authors declare no competing financial interest.

ACKNOWLEDGMENTS

We gratefully acknowledge financial support from the National Science Foundation (CHE 2102049).

REFERENCES

- (1) Howard, P.; Morris, G.; Sunley, G. In *Metal-Catalysis in Industrial Organic Processes*; Chiusoli, G. P., Maitlis, P. M., Eds.; Royal Society of Chemistry, 2006; pp 1–22.
- (2) Bullock, R. M.; Chen, J. G.; Gagliardi, L.; Chirik, P. J.; Farha, O. K.; Hendon, C. H.; Jones, C. W.; Keith, J. A.; Klosin, J.; Minteer, S. D.; Morris, R. H.; Radosevich, A. T.; Rauchfuss, T. B.; Strotman, N. A.; Vojvodic, A.; Ward, T. R.; Yang, J. Y.; Surendranath, Y. Using nature's blueprint to expand catalysis with Earth-abundant metals. *Science* 2020, 369, eabc3183.
- (3) Chirik, P. J.; Wieghardt, K. Radical Ligands Confer Nobility on Base-Metal Catalysts. *Science* **2010**, 327, 794–795.
- (4) Bart, S. C.; Lobkovsky, E.; Chirik, P. J. Preparation and molecular and electronic structures of iron(0) dinitrogen and silane complexes and their application to catalytic hydrogenation and hydrosilation. *J. Am. Chem. Soc.* **2004**, *126*, 13794–13807.
- (5) Bouwkamp, M. W.; Bowman, A. C.; Lobkovsky, E.; Chirik, P. J. Iron-Catalyzed [2pi + 2pi] Cycloaddition of alpha,omega-Dienes: The Importance of Redox-Active Supporting Ligands. *J. Am. Chem. Soc.* **2006**, *128*, 13340–13341.
- (6) Guo, J.; Cheng, Z.; Chen, J.; Chen, X.; Lu, Z. Iron- and Cobalt-Catalyzed Asymmetric Hydrofunctionalization of Alkenes and Alkynes. *Acc. Chem. Res.* **2021**, *54*, 2701–2716.
- (7) Elsby, M. R.; Baker, R. T. Strategies and mechanisms of metalligand cooperativity in first-row transition metal complex catalysts. *Chem. Soc. Rev.* **2020**, *49*, 8933–8987.
- (8) Berben, L. A. Toward Acetylide and N-Hetercycle-Bridged Materials with Strong Electronic and Magnetic Coupling. Ph.D. Dissertation, University of California, Berkeley, 2005.
- (9) Hoffert, W. A.; Kabir, M. K.; Hill, E. A.; Mueller, S. M.; Shores, M. P. Stepwise acetylide ligand substitution for the assembly of ethynylbenzene-linked Co(III) complexes. *Inorg. Chim. Acta* **2012**, 380, 174–180.

- (10) Thakker, P. U.; Aru, R. G.; Sun, C.; Pennington, W. T.; Siegfried, A. M.; Marder, E. C.; Wagenknecht, P. S. Synthesis of trans bis-alkynyl complexes of Co(III) supported by a tetradentate macrocyclic amine: A spectroscopic, structural, and electrochemical analysis of pi-interactions and electronic communication in the C equivalent to C-M-C equivalent to C structural unit. *Inorg. Chim. Acta* 2014, 411, 158–164.
- (11) Ren, T. A Sustainable Metal Alkynyl Chemistry: 3d Metals and Polyaza Macrocyclic Ligands. *Chem. Commun.* **2016**, 52, 3271–3279.
- (12) Clendening, R. A.; Ren, T. Mono- and Bis-alkynyl Iron Complexes Supported by a "Softened" Tetraaza Macrocycle. *Eur. J. Inorg. Chem.* **2022**, 2022, e202101021.
- (13) Clendening, R. A.; Zeller, M.; Ren, T. Bis-Alkynyl Complexes of Fe(III) Tetraaza Macrocycles A Tale of Two Rings. *Inorg. Chem.* **2022**, *61*, 13442–13452.
- (14) Hess, C. R.; Weyhermuller, T.; Bill, E.; Wieghardt, K. Influence of the Redox Active Ligand on the Reactivity and Electronic Structure of a Series of Fe(TIM) Complexes. *Inorg. Chem.* **2010**, 49, 5686–5700.
- (15) Rodriguez Segura, L.; Ren, T. Formation of an aza-cobalt-cyclobutene on CoIII(TIM): Hidden Noninnocence of the TIM ligand. *Organometallics* **2022**, *41*, 1130–1133.
- (16) Walsh, P. J.; Hollander, F. J.; Bergman, R. G. Generation, alkyne cycloaddition, arene carbon-hydrogen activation, nitrogen-hydrogen activation and dative ligand trapping reactions of the first monomeric imidozirconocene (Cp2Zr:NR) complexes. *J. Am. Chem. Soc.* 1988, 110, 8729–8731.
- (17) Walsh, P. J.; Baranger, A. M.; Bergman, R. G. Stoichiometric and catalytic hydroamination of alkynes and allene by zirconium bisamides Cp2Zr(NHR)2. *J. Am. Chem. Soc.* **1992**, *114*, 1708–1719.
- (18) Vaughan, G. A.; Hillhouse, G. L.; Rheingold, A. L. Syntheses, structures, and reactivities of unusual four-membered metallacycles formed in insertion reactions of N:N:O, N:N:NR, and N:N:CR2 with (.eta.5-C5Me5)2Zr(C2Ph2). *J. Am. Chem. Soc.* **1990**, *112*, 7994–8001.
- (19) Ward, B. D.; Maisse-Francois, A.; Mountford, P.; Gade, L. H. Synthesis and structural characterization of an azatitanacyclobutene: the key intermediate in the catalytic anti-Markovnikov addition of primary amines to a-alkynes. *Chem. Commun.* **2004**, 704–705.
- (20) Polse, J. L.; Andersen, R. A.; Bergman, R. G. Reactivity of a Terminal Ti(IV) Imido Complex toward Alkenes and Alkynes: Cycloaddition vs C-H Activation. *J. Am. Chem. Soc.* **1998**, *120*, 13405–13414.
- (21) Fischer, M.; Wolff, M. C.; del Horno, E.; Schmidtmann, M.; Beckhaus, R. Synthesis, Reactivity, and Insights into the Lewis Acidity of Mononuclear Titanocene Imido Complexes Bearing Sterically Demanding Terphenyl Moieties. *Organometallics* **2020**, *39*, 3232–3239
- (22) Richards, C. A.; Rath, N. P.; Neely, J. M. Isolation and Reactivity of an Iron Azametallacyclobutene Complex. *Organometallics* **2022**, *41*, 1763–1768.
- (23) Richards, C. A.; Rath, N. P.; Neely, J. M. Carbene-Like Reactivity in an Iron Azametallacyclobutene Complex: Insights from Electronic Structure. *Inorg. Chem.* **2022**, *61*, 13266–13270.
- (24) Rodriguez Segura, L.; Lee, S. A.; Mash, B. L.; Schuman, A. J.; Ren, T. A Series of Mono- and Bis-Alkynyl Co(III) Complexes Supported by a Tetra-imine Macrocyclic Ligand (TIM). *Organo-metallics* **2021**, *40*, 3313–3322.
- (25) Zhang, J.; Guo, S.-Z.; Dong, Y.-B.; Rao, L.; Yin, J.; Yu, G.-A.; Hartl, F.; Liu, S. H. Multistep Oxidation of Diethynyl Oligophenylamine-Bridged Diruthenium and Diiron Complexes. *Inorg. Chem.* **2017**, *56*, 1001–1015.
- (26) Heyer, E.; Ziessel, R. Panchromatic Push-Pull Dyes of Elongated Form from Triphenylamine, Diketopyrrolopyrrole, and Tetracyanobutadiene Modules. *SynLett.* **2015**, *26*, 2109–2116.
- (27) Banziger, S. D.; Raghavan, A.; Zeller, M.; Ren, T. Co(cyclam) Complexes of Triarylamine-acetylide: Structural and Spectroscopic Properties and DFT Analysis. *Organometallics* **2020**, *39*, 3250–3259.

- (28) Cuffe, L.; Hudson, R. D. A.; Gallagher, J. F.; Jennings, S.; McAdam, C. J.; Connelly, R. B. T.; Manning, A. R.; Robinson, B. H.; Simpson, J. Synthesis, Structure, and Redox Chemistry of Ethenyl and Ethynyl Ferrocene Polyaromatic Dyads. *Organometallics* **2005**, *24*, 2051–2060.
- (29) Sheridan, M. V.; Lam, K.; Sharafi, M.; Schneebeli, S. T.; Geiger, W. E. Anodic Methods for Covalent Attachment of Ethynylferrocenes to Electrode Surfaces: Comparison of Ethynyl Activation Processes. *Langmuir* **2016**, 32, 1645–1657.
- (30) Krejcik, M.; Danek, M.; Hartl, F. Simple construction of an infrared optically transparent thin-layer electrochemical cell: Applications to the redox reactions of ferrocene, Mn2(CO)10 and Mn(CO)3(3,5-di-t-butyl-catecholate)-. *J. Electroanal. Chem.* **1991**, 317, 179–187.
- (31) Mash, B. L. Tuning the Electronic Properties of Cyclam Derivatives: Enhanced Intermetallic Coupling and Catalysis. Ph.D. Dissertation, Purdue University, 2020.
- (32) Jakob, A.; Ecorchard, P.; Linseis, M.; Winter, R. F.; Lang, H. Synthesis, solid state structure and spectro-electrochemistry of ferrocene-ethynyl phosphine and phosphine oxide transition metal complexes. *J. Organomet. Chem.* **2009**, 694, 655–666.
- (33) Whitehurst, W. G.; Kim, J.; Koenig, S. G.; Chirik, P. J. C-H activation by isolable cationic bis(phosphine) cobalt(III) metallacycles. *J. Am. Chem. Soc.* **2022**, *144*, 19186–19195.
- (34) Esezobor, O. Z.; Zeng, W.; Niederegger, L.; Grubel, M.; Hess, C. R. Co–Mabiq Flies Solo: Light-Driven Markovnikov-Selective C-and N-Alkylation of Indoles and Indazoles without a Cocatalyst. *J. Am. Chem. Soc.* **2022**, *144*, 2994–3004.
- (35) Occhialini, G.; Palani, V.; Wendlandt, A. E. Catalytic, contra-Thermodynamic Positional Alkene Isomerization. *J. Am. Chem. Soc.* **2002**, *144*, 145–152.
- (36) Deacy, A. C.; Phanopoulos, A.; Lindeboom, W.; Buchard, A.; Williams, C. K. Insights into the Mechanism of Carbon Dioxide and Propylene Oxide Ring-Opening Copolymerization Using a Co(III)/K(I) Heterodinuclear Catalyst. *J. Am. Chem. Soc.* **2022**, *144*, 17929–17938.
- (37) Jackels, S. C.; Farmery, K.; Barefield, E. K.; Rose, N. J.; Busch, D. H. Tetragonal cobalt(III) complexes containing tetradentate macrocyclic amine ligands with different degrees of unsaturation. *Inorg. Chem.* **1972**, *11*, 2893–2901.
- (38) Planells, M.; Abate, A.; Hollman, D. J.; Stranks, S. D.; Bharti, V.; Gaur, J.; Mohanty, D.; Chand, S.; Snaith, H. J.; Robertson, N. Diacetylene bridged triphenylamines as hole transport materials for solid state dye sensitized solar cells. *J. Mater. Chem. A* **2013**, *1*, 6949–6960
- (39) SHELXTL Suite of Programs, version 6.14; Bruker AXS Inc.: Madison, WI, 2000–2003.
- (40) Hübschle, C. B.; Sheldrick, G. M.; Dittrich, B. ShelXle: a Qt graphical user interface for SHELXL. *J. Appl. Crystallogr.* **2011**, *44*, 1281–1284.
- (41) Sheldrick, G. M. Crystal structure refinement with SHELXL. *Acta Crystallogr. C* **2015**, 71, 3–8.